PHYSICAL REVIEW A

GENERAL PHYSICS

THIRD SERIES, VOL. 4, NO. 4 OCTOBER 1971

Radiative Lifetime of the 2 $^1S_0$ Metastable State of Helium†

Robert S. Van Dyck, Jr., * Charles E. Johnson, and Howard A. Shugart
Department of Physics and Lawrence Radiation Laboratory, University of California, Berkeley, California 94720
(Received 21 May 1971)

A time-of-flight technique has been used to measure the radiative lifetime of the $2\,^1S_0$ state of helium. After passing from a cooled source, helium atoms are excited by a pulsed antiparallel electron beam. The atomic beam then contains not only ground-state helium atoms but also metastable atoms in both the $2\,^3S_1$ and the $2\,^1S_0$ states. The metastable atoms are detected at two positions, 1.9 and 6.7 m from the electron gun, by Auger ejection of an electron from a copper target, the first of which is a 60% transmitting mesh. Ground-state helium atoms cannot cause an electron to be ejected and hence are not detected. The time-of-flight distribution for the metastable $2\,^1S_0$ state is separated from that of the $2\,^3S_1$ state by illuminating the beam with an rf-discharge helium lamp. The $2\,^1S_0$ state is quenched by resonant absorption of a 20 581-Å photon, raising the atom to the $2\,^1P_1$ state, which then decays preferentially to the $^1S_0$ ground state; the $2\,^3S_1$ state remains unaffected because it is the ground state for the triplet system. The time-of-flight distribution for the $2\,^1S_0$ atoms is therefore obtained from the difference between the full beam and the quenched beam. A comparison of the number of $2\,^1S_0$ metastables within a given velocity interval at the two detectors determines the number which decay in flight and yields a value for the two-photon radiative lifetime. The value of the singlet lifetime for both He^3 and He^4 is 19.7 ± 1.0 msec, agreeing with the theoretical value of 19.5 msec, but disagreeing with the value 38 ± 8 msec measured by Pearl using a movable detector. The 1.0-msec error is an estimate of the remaining systematic errors in the experiment.

I. INTRODUCTION

A metastable state of any atom was once thought to exist for a very long time, only being able to change state through collisions, absorption of radiation, or perturbation by external fields. The appearance of forbidden lines, originally thought to belong to unidentified elements, initiated a large amount of both experimental and theoretical work on possible secondary decay mechanisms. The early pioneering work involved the unidentified lines from planetary nebulae, the sun's corona, and the polar aurora. Bowen,[1] for example, found that some unidentified lines from nebulae were the forbidden lines of O I, N II, and O III, while the lines in the aurora were forbidden lines of O I. Today most of the "forbidden" lines have been examined and found to arise from transitions between two energy levels of known atoms or their multiply ionized states. These observations provided scientists with solid evidence for the existence of second-order multipole radiation, i.e., electric quadrupole and magnetic dipole, where before only electric dipole radiation had been considered. With this new attention on secondary decay mechanisms, Goeppert-Mayer[2] developed a theory of multiple quanta radiation. In 1940, Breit and Teller[3] predicted the lifetime of the metastable $^2S_{1/2}$ state of hydrogen, based on a two-photon decay process, to be 143 msec. Since the $2\,^1S_0$ metastable state of helium also decays by two-photon emission, they estimated the lifetime of this state to be approximately the same; however, the lifetime of the $2\,^3S_1$ metastable state was expected to be much longer.

Forbidden radiation is of interest to astrophysicists, since metastable states of atoms provide much of the light emitted from planetary nebulae, where the density of matter is tenuous ($\approx$1000 atoms/cm^3). Atoms can therefore exist a long time before making collisions and, provided the radiation density is not too large, will live long enough to decay spontaneously, emitting forbidden radiation. Mea-

suring the intensity of these forbidden lines yields information concerning the density, temperature, chemical composition, and other important properties of these nonterrestrial features. For instance, the two-photon decay of the $2\,^2S_{1/2}$ metastable state of hydrogen is used to explain the continuous emission spectra of the planetary nebulae.[4] Also, metastable helium is quite abundant in the atmospheres of certain Be stars and can be used for studying various properties of these stars.[5]

The first laboratory evidence[6] of the two-photon emission process was observed in 1965 with an experiment on the $2\,^2S_{1/2}$ state of He^+. Using an angular correlation technique, coincidence counts were collected by two independent counters with an angle θ between them. The counts were shown to be correlated with an angular dependence according to $1+\cos^2\theta$, as expected[7] for this two-photon decay.

The two-photon decay process is also of fundamental importance to theoreticians. The lifetime of a metastable state which decays by two-photon emission is very sensitive to the exact wave functions describing states that are connected to the metastable state by electric dipole radiation. Until the last five years, though, most interest in the two-photon decay process concentrated on the $2\,^2S_{1/2}$ state of hydrogenlike systems. Then, in 1966, Dalgarno[8] published his first estimate of the lifetime of the $2\,^1S_0$ metastable state of helium, utilizing sum rules of oscillator strengths that had been determined experimentally and theoretically. The lifetime obtained was 22 msec. Later, Dalgarno and Victor[9] calculated the lifetime to be 12 msec, using a special sum rule with initial- and final-state wave functions obtained from the time-dependent uncoupled Hartree-Fock approximation; this is a simpler but less accurate method of calculation. In 1967, Victor[10] calculated a value of 20 msec using wave functions obtained from the time-dependent coupled Hartree-Fock approximation. The most recent and most accurate calculation by Drake, Victor, and Dalgarno[11] gives $\tau(2\,^1S_0)=19.5$ msec. In this calculation, correlation-type wave functions are used, in which the positions of the two electrons are correlated by including a dependence on the distance between electrons. Recently Jacobs[12] also completed an independent calculation using both length and velocity matrix elements; he obtains a value of $\tau(2\,^1S_0)=19.6$ msec.

The first beam experiment[13] to measure the metastable helium lifetime yielded only a lower limit for the $2\,^1S_0$ lifetime. Steinberg's apparatus was an earlier version of the present experiment and utilized the same time-of-flight technique for determining lifetimes. His apparatus was, however, severely pressure limited and was only capable of measuring a lower limit of 9 msec for the $2\,^1S_0$ lifetime. Pearl[14] used a single movable detector to report an experimental determination of the $2\,^1S_0$ lifetime. His value of 38 ± 8 msec, however, seriously disagrees not only with the theoretical result[11] of 19.5 msec but also with our present experiment, as reported previously.[15] Following a discussion of the helium metastable states, this paper outlines the theory of two-photon decay, analyzes the time-of-flight technique for measuring metastable lifetimes, and explains the apparatus and data analysis used to obtain an experimental result for the two-photon radiative lifetime of the $2\,^1S_0$ metastable state.

II. HELIUM METASTABLE STATES

The lowest-lying energy levels of helium are shown in Fig. 1. The only transition possible for the $2\,^3S_1$ state is to the $1\,^1S_0$ ground state. An examination of the selection rules[16] shows, however, that the $2\,^3S_1$ state is metastable and is therefore effectively the ground state of the triplet system. The transition is forbidden for electric dipole radiation since the parity does not change; electric quadrupole radiation is also forbidden for a $J=1\rightarrow J=0$ transition. Although the transition does satisfy the rigorous selection rules for magnetic dipole radiation, the selection rule $\Delta S=0$ would be violated. This rule holds well for helium since LS coupling is an excellent approximation. The most probable decay mode for the $2\,^3S_1$ state would therefore appear to be two-photon emission. In fact, for many years after the discovery of forbidden lines, it was thought that the $2\,^3S_1\rightarrow 1\,^1S_0$ transition could occur only by two-photon emission with

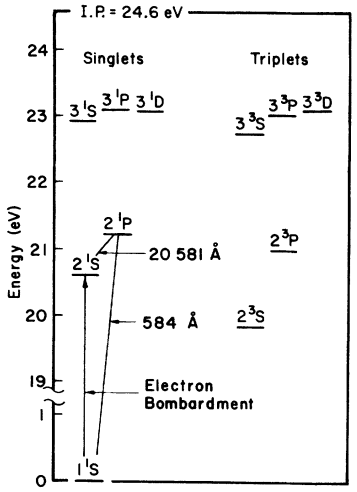

FIG. 1. Lowest helium energy levels. The $2\,^1S_0$ metastable state is produced by electron bombardment of the $1\,^1S_0$ ground state. Quenching of the $2\,^1S_0$ state occurs by resonant absorption to the $2\,^1P_1$ state, which decays preferentially to the ground state.

a transition probablilty between 10^{-8} and 10^{-9} $\sec^{-1}$. However, there are spin-dependent relativistic correction operators to the usual magnetic dipole operator which allow a nonzero relativistic magnetic dipole transition to exist directly between the $2\,^3S_1$ state and the $1\,^1S_0$ ground state. The corresponding transition probability for this decay mode has been calculated[17] to be about 10^{-4} $\sec^{-1}$. The $2\,^3S_1$ metastable state should therefore decay by relativistic magnetic dipole radiation rather than by two-photon emission.

The $2\,^1S_0$ state lies above both the $2\,^3S_1$ and the $1\,^1S_0$ states. The intercombination transition $2\,^1S_0 \rightarrow 2\,^3S_1$ violates the $\Delta S = 0$ selection rule and is consequently very improbable. The only other possibility, the $2\,^1S_0 \rightarrow 1\,^1S_0$ transition, is a $J = 0 \rightarrow J = 0$ transition, which is rigorously forbidden for all orders of single-photon multipole radiation. The next most probable decay mechanism available for the $2\,^1S_0$ state is the emission of two electric dipole photons. The object of this research is to determine experimentally the mean life of this state. Since the calculated $2\,^1S_0$ lifetime of 19.5 msec is very short when compared to the expected $2\,^3S_1$ lifetime of 10^4 sec, the $2\,^3S_1$ state can, for the purposes of this experiment, be considered to have an essentially infinite lifetime.

III. THEORETICAL TWO-PHOTON LIFETIME

The expression[3] for the probability of emitting two photons spontaneously, with one photon having a frequency between ν_1 and $\nu_1 + d\nu_1$, is

$$A(\nu_1)\,d\nu_1 = \frac{2^{10}\pi^6 e^4}{h^2 c^6}\ \nu_1^3\,\nu_2^3\,|M_{fi}|^2_{\rm av}\,d\nu_1\ , \qquad (1)$$

where, by conservation of energy,

$$E = h\nu_1 + h\nu_2 = E_i - E_f\ ;$$

E is the energy difference between the initial state i and final state f. The matrix element M_{fi} for the transition must be averaged over the directions of propagation and of polarization $\hat{\epsilon}$, independently for both photons. The matrix element M_{fi} for two electric dipole photons is

$$M_{fi} = \sum_n \left(\frac{(\hat{\epsilon}_1 \cdot \vec{r})_{fn}\,(\hat{\epsilon}_2 \cdot \vec{r})_{ni}}{\nu_{ni} + \nu_2} + \frac{(\hat{\epsilon}_2 \cdot \vec{r})_{fn}\,(\hat{\epsilon}_1 \cdot \vec{r})_{ni}}{\nu_{ni} + \nu_1} \right) . \qquad (2)$$

Energy $h\nu_{ni}$ is the difference between intermediate and initial state energies. The summation over n includes all possible real intermediate states of the atom, as well as states in the continuum. Since matrix elements representing allowed electric dipole transitions are much larger than those representing other decay modes, the intermediate states must be only those which can be reached from the initial state, and also the final state, by absorption of a single electric dipole photon. This criterion is satisfied for an initial $2\,^1S_0$ state and a final $1\,^1S_0$ state by the $n\,^1P$ states, which are therefore the ones to enter the summation over n. Thus, terms like $(\hat{\epsilon}_1 \cdot \vec{r})_{fn}$ are the usual electric dipole matrix elements between the $^1S_0$ and $n\,^1P$ states in which $\vec{r}$ is the sum of the position vectors of the two electrons.

Equation (2) can be shown[3] to reduce to

$$M_{fi} = (\hat{\epsilon}_1 \cdot \hat{\epsilon}_2) \sum_{n=2} z_{fn} z_{ni} \left(\frac{1}{\nu_{ni} + \nu_2} + \frac{1}{\nu_{ni} + \nu_1} \right) ,$$

where the index n refers to the intermediate ^1P state, and z_{fn} and z_{ni} are the electric dipole matrix elements between the $^1S_0$ and ^1P states. The relationship between the directions of polarization of the two photons is given by $(\hat{\epsilon}_1 \cdot \hat{\epsilon}_2)$; thus the emission probability is proportional to $\cos^2\theta$ of the angle between the two polarization directions. The necessary average over polarization directions is

$$(1/4\pi) \int \cos^2\theta\, d\Omega = \tfrac{1}{3}\ .$$

Equation (1) therefore becomes

$$A(\nu_1)\,d\nu_1 = \frac{2^{10}\pi^6 e^4}{3h^2 c^6}\ \nu_1^3\,\nu_2^3 \times \left[\sum_{n=2} z_{fn} z_{ni} \left(\frac{1}{\nu_{ni} + \nu_1} + \frac{1}{\nu_{ni} + \nu_2} \right) \right]^2 d\nu_1\ , \qquad (3)$$

where the summation is understood to include the continuum. Equation (3) is the starting point for most theoretical calculations[8-12] of the $2\,^1S_0$ lifetime. The various calculations have differed in the choice of wave functions used to calculate the matrix elements z_{fn} and z_{ni}.

The total two-photon emission probability A_T is obtained by integrating Eq. (3) over frequency ν_1:

$$A_T = \tfrac{1}{2} \int_0^{E/h} A(\nu_1)\,d\nu_1\ ,$$

where the factor $\frac{1}{2}$ results from counting photon 1 twice in the frequency interval $[0, E/h]$. The mean life for two-photon emission is then

$$\tau(2\,^1S_0) = 1/A_T\ .$$

IV. TIME-OF-FLIGHT ANALYSIS

The formalism for the time-of-flight technique is first outlined for the general case of an atomic beam containing different metastable states created instantaneously by a pulsed electron beam at a single position; then the theory is applied to the case of helium, showing how the lifetime τ of the $2\,^1S_0$ state can be determined.

A. General Formalism

The number of atoms in a particular metastable

state k with initial velocity distribution $n_0(v,k)$, which arrive at detector i at time t_i, is $n_0(v,k) \times e^{-t_i/\tau_k}$; the exponential factor allows for the possibility of radiative decay with mean life τ_k. The probability of detecting a particular metastable atom depends upon the surface efficiency $\epsilon_i(k)$ of detector i. Although this efficiency should be velocity independent for the thermal velocity range of this experiment, it is not necessarily true that the efficiency is independent of position on the detector surface. The total number $N_i(v)$ of metastable atoms with velocity v that are counted at detector i is therefore obtained not only by summing over the different metastable states k, but also by integrating over the surface of the detector:

$$N_i(v) = \sum_k \int_{\text{surface}} \epsilon_i(k)\, n_0(v,k)\, e^{-t_i/\tau_k}\, dS \,. \tag{4}$$

Dependence on the details of the detector surface is eliminated by ensuring that the initial velocity distribution $n_0(v,k)$ is uniform across the beam so that each point on the detector surface sees the same velocity distribution. The number of metastable atoms counted is then simply

$$N_i(v) = \sum_k C_i(k)\, n_0(v,k)\, e^{-t_i/\tau_k} \,, \tag{5}$$

where $C_i(k) = \int_{\text{surface}} \epsilon_i(k)\, dS$ is a constant efficiency factor of the ith detector. A comparison of the number of metastable atoms in the same velocity interval at two spatially separated detectors allows the determination of the mean lifetimes τ_k, since, with the reasonable assumption that the velocity distribution $n_0(v,k)$ is the same for all states k, the ratio

$$R = \frac{N_2(v)}{N_1(v)} = \frac{\sum_k C_2(k)\, e^{-t_2/\tau_k}}{\sum_k C_1(k)\, e^{-t_1/\tau_k}} \tag{6}$$

is independent of this velocity distribution. The ratio is also evidently independent of the initial velocity distribution if only one metastable state is present in the beam, and

$$R = \frac{N_2(v)}{N_1(v)} = \frac{C_2\, e^{-t_2/\tau}}{C_1\, e^{-t_1/\tau}} = C e^{-t/\tau} \,, \tag{7}$$

where $t = t_2 - t_1$ is the time of flight between the two detectors. The natural logarithm of Eq. (7) yields the equation of a straight line whose slope is $-1/\tau$.

B. Metastable Helium Analysis

Since the $2\,^3S_1$ level in helium is lower in energy than the $2\,^1S_0$ level, electron bombardment excitation necessarily produces atoms in both metastable states. Atoms in the $2\,^1S_0$ state can be quenched, however, by exciting them with 20 581-Å resonance radiation to the $2\,^1P_1$ state, which subsequently decays preferentially to the $^1S_0$ ground state by emitting 584-Å radiation (see Fig. 1). Application of Eq. (5) to the specific case of helium shows that the number of counts at the first detector with the quench lamp off is

$$N_1(\text{off}) = C_1(^1S)\, n_0(^1S)\, e^{-t_1/\tau_1} + C_1(^3S)\, n_0(^3S)\, e^{-t_1/\tau_3} \,. \tag{8}$$

If the quench radiation is not 100% effective, then only a certain fraction $f(v)$ of the $2\,^1S_0$ atoms are quenched, where $f(v)$ may depend on the velocity of the atom. Again applying Eq. (5), but now with the quench lamp on, gives

$$N_1(\text{on}) = [1 - f(v)]\, C_1(^1S)\, n_0(^1S)\, e^{-t_1/\tau_1} + C_1(^3S)\, n_0(^3S)\, e^{-t_1/\tau_3} \tag{9}$$

as the number of metastable atoms counted at the first detector. The difference between Eqs. (8) and (9) is the effective number of $2\,^1S_0$ metastable atoms which are analyzed to determine the mean life τ_1:

$$N_1(^1S) \equiv N_1(\text{off}) - N_1(\text{on}) = C_1(^1S)\, f(v)\, n_0(^1S)\, e^{-t_1/\tau_1} .$$

Similarly, for the second detector,

$$N_2(^1S) = C_2(^1S)\, f(v)\, n_0(^1S)\, e^{-t_2/\tau_1} .$$

The ratio of the number of atoms counted within the same velocity interval is not only independent of the initial velocity distribution $n_0(v)$, but is also independent of the details of the quenching process as contained in the quenching fraction $f(v)$. The logarithm of this ratio is

$$\ln R \equiv \ln\left[\frac{N_2(^1S)}{N_1(^1S)}\right] = A - \frac{t}{\tau_1} \,, \tag{10}$$

where $t = t_2 - t_1$ is the time of flight for a particular velocity interval and A is a constant depending on the efficiency of the two detectors. The calculation of this ratio for several different velocity intervals of the time-of-flight distribution allows a determination of the mean life from the slope $= -1/\tau_1$ of a straight line, least-squares fitted to plot of $\ln R$ versus the time of flight.

V. APPARATUS

The time-of-flight apparatus is outlined in Fig. 2. The major components in addition to the vacuum system are (A) the source, (B) the metastabilizer (electron gun), (C) the quench lamp, and (D) the detector at either end of a 4.8-m drift region. Cooled helium gas effuses from the source and passes vertically through the metastabilizer where a pulsed antiparallel electron beam excites the ground-state atoms to the two metastable states. The resonance discharge lamp allows the effective separation of the $2\,^1S_0$ and $2\,^3S_1$ metastable states. A comparison of the number of $2\,^1S_0$ metastable atoms within specific velocity intervals arriving at the two detectors yields the number which decay in flight between them, and consequently gives the

mean life τ of the $2\,^1S_0$ state. The major components will now be described in more detail.

A. Vacuum System

The nature of a time-of-flight experiment for measuring the lifetime of a metastable state requires that the loss of metastable atoms between the two detectors resulting from residual gas scattering be negligible in comparison to the loss from radiative decay. To achieve this situation the vacuum system is constructed of stainless steel and, following a 48-h bakeout at 300 °C, a pressure in the drift region of 1×10^{-10} Torr is obtainable with liquid-nitrogen trapping. Experimentally, a drift-region pressure lower than 1×10^{-8} Torr proved sufficient to eliminate any systematic scatting effect on the lifetime, and all final data were taken with the pressure this low or lower.

An additional requirement of the vacuum system is that there be sufficient buffer chambers and pumping speed to ensure that the drift-region pressure does not increase while a helium beam is flowing. The present apparatus has three buffer chambers; the first is pumped by a 2000-liter/sec oil diffusion pump, the second and third by 500-liter/sec liquid-nitrogen-trapped pumps. The drift region is pumped by three equally spaced 1000-liter/sec pumps. No detectable rise in drift-region pressure was observed even for a helium flow rate 100 times that used during data collection.

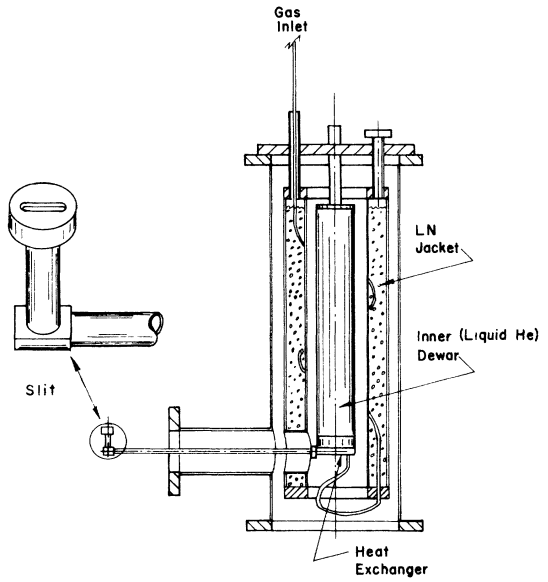

FIG. 3. Source assembly. The helium gas effusing from the slit can be cooled by either liquid nitrogen or liquid helium

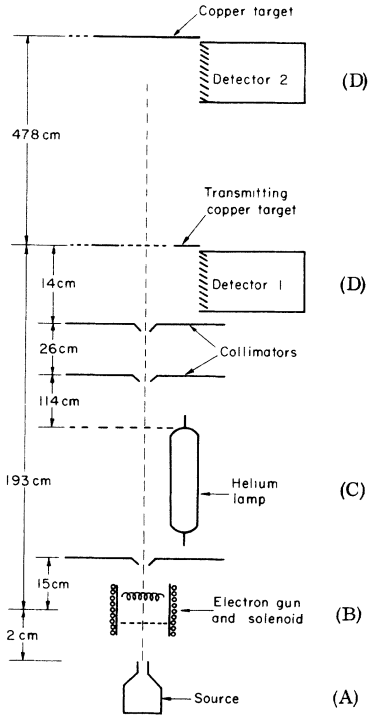

FIG. 2. Apparatus outline. Ground-state atoms effuse from the source (A) and are excited to the $2\,^1S_0$ and $2\,^3S_1$ metastable states by electron bombardment (B). The $2\,^1S_0$ state can be quenched by the discharge lamp (C), and the metastable atoms are detected (D) at both ends of the time-of-flight region.

The stainless-steel plates, each with a 0.64-cm axial hole, separating the various buffer chambers also served as collimators. The main purpose of the collimation and subsequent lineup of the source slit, electron gun, and collimators is to assure that any atom that can be seen by the lower detector can also be seen by the upper detector. The source area, in the worst possible situation, is determined only by the collimator directly above the electron gun. Then the linear dimension subtended across the lower detector is 0.74 cm and the corresponding dimension on the upper detector is 4.45 cm. Since each detector target has a minimum dimension of 9.0 cm, both detectors necessarily see the same metastable beam.

The collimators also eliminate helium ions from the beam; an ion moving through the earth's magnetic field must have a velocity greater than 70 000 m/sec to pass through the collimators and reach the first detector. However, only $2\,^1S_0$ metastable atoms with velocities less than 2000 m/sec are detected in a quantity sufficient for data analysis. The maximum solid angle subtended by the beam is 5×10^{-5} sr and indicates that the number of uv photons reaching the detectors from the quench region is negligible in comparison to the metastable beam.

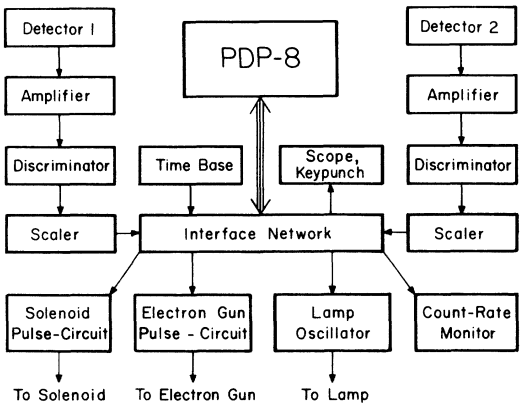

FIG. 4. Data collection and storage. The PDP-8 computer stores metastable atom counts from both detectors in channels whose width is determined by the time-base oscillator. The PDP-8 also controls the electron gun and solenoid pulses, and gates the lamp on-off at the appropriate times.

B. Source

Commercial-grade helium is stored in a 10-liter volume at atmospheric pressure. The gas flow from the reservoir to the source assembly is controlled by a needle valve. A typical flow rate is 0.1 liter/h and is very stable during a 2-h run.

The source assembly, shown in Fig. 3, is used to cool the helium. The inner Dewar of this assembly can be filled with either liquid nitrogen or liquid helium, and the outer jacket normally contains liquid nitrogen. The source gas is first cooled to liquid-nitrogen temperature inside this outer jacket before passing into the heat exchanger attached to the bottom of the inner Dewar. A long copper tube is attached to this heat exchanger to bring the cooled gas to the beam axis. When liquid helium is used, a radiation shield at liquid-nitrogen temperature is placed over the long copper tube. The 0.025-cm-wide slit at the end of this tube is oriented parallel to the direction of the tube and is 0.5 cm long. The pressure in the source tube is about 0.05 Torr for a flow rate of 0.1 liter/h.

C. Metastabilizer

Ground-state helium atoms are excited to the $2\,^1S_0$ metastable state by electron bombardment immediately after the source slit. The electron gun is a type of sheath electrode gun described previously.[18] The atomic beam passes antiparallel to the electron beam through a 2×0.25-cm slot in the collector and between the two side electrodes which define the 1-cm-long excitation region. The electron beam originates from a 2.5-cm-long, 0.025-cm-diam thoriated tungsten filament heated by about 8 A of 3-kHz audio-frequency current; about 20 mA of emission current are obtained at 50 V. A 300-G magnetic field from a concentric solenoid helps focus the electrons onto the collector and confine them to the excitation region.

D. Quench Lamp

An air-cooled rf-discharge helium lamp[19] is located adjacent to the first buffer chamber and illuminates the metastable beam through a Pyrex window. The lamps are made from an 8-cm-long, 0.8-cm-diam Pyrex tube, and are prepared with special emphasis on cleanliness and purity of the gas sample. The lamps are evacuated and baked before filling to about 5 Torr. A 50-W, 70-MHz oscillator drives the lamp.

E. Detection System

The basic goal of the detection system is to preferentially detect the metastable atoms and to store the data for both detectors according to time of flight. When a metastable atom strikes a copper detector target, the first being a 60% transparent electroformed mesh, the ejected Auger electron is focused onto an electron multiplier. The resultant pulse is amplified, counted, and then stored in a PDP-8 computer memory location corresponding to its arrival time after the initial electron gun pulse. A block diagram of the total data collection network is shown in Fig. 4. The central component of this network is the PDP-8 digital computer, programmed to control the solenoid and gun-pulsing circuits, the lamp oscillator circuit, the output keypunch, and the data storage. The interface network properly gates and registers the count

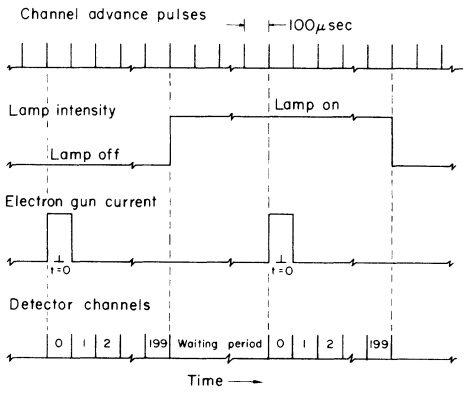

FIG. 5. Timing scheme. Channel advance pulses from a crystal-controlled oscillator determine the channel width and furnish the PDP-8 computer with synchronizing pulses for control of the electron gun, solenoid, and quench lamp. The solenoid current is pulsed on for a few milliseconds before channel 0, which is the electron gun on time. The lamp is switched on-off for alternate data collection cycles.

rate for lamp on and lamp off, gating out light pulses received when the electron gun is on.

The timing aspects of the experiment are shown in Fig. 5. A crystal-controlled oscillator supplies the channel advance pulses, which the PDP-8 uses as a reference to determine the proper sequence of events. Channel 0 corresponds to the duration of the electron gun pulse and the creation of a pulse of metastable atoms. Time $t = 0$ is at the center of channel 0. The focusing solenoid is pulsed on a few milliseconds before channel 0 and is turned off at the end of the gun pulse. To improve the lamp's stability while data counts are being collected, the lamp is turned on or off at the beginning of a 16-msec waiting period. This period is the time the PDP-8 needs for adding data collected in buffer registers to that already stored from previous sweeps. Data counts are collected at both detectors simultaneously with a total number of about 10^7 metastable atoms counted during a 2-h run; most runs were for 4 h, though several 12-h runs were taken. The longer runs allowed sufficient counts to accumulate in the tail of the distribution so that longer flight times could be included in the analysis.

VI. DATA ANALYSIS

As displayed by the interface oscilloscope, an example of the data collected and stored by the PDP-8 computer during a run is shown in Fig. 6; the first two time-of-flight distributions correspond, respectively, to detector 1 and detector 2 with the quench lamp off, while the last two correspond to those with the lamp on. Essentially, metastable atom pulses from both detectors are counted simultaneously for equally wide time-sequenced

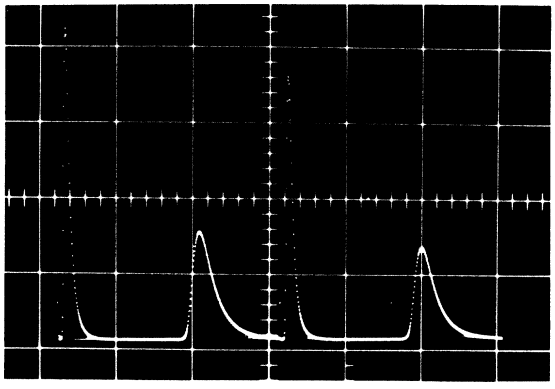

FIG. 6. Interface oscilloscope display. The first half of the display, consisting of 200 80-μsec-wide channels for each detector, corresponds to the quench lamp off, while the second 400 channels are with the lamp on. The decrease in peak height represents the $2\,^1S_0$ metastable atoms that are quenched by the discharge lamp. The vertical scale is about 10^5 counts/cm.

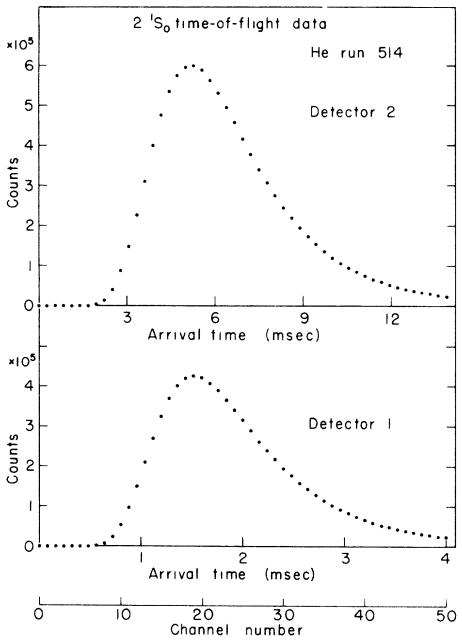

FIG. 7. Time-of-flight distributions. Appropriate data analysis yields the time-of-flight distributions for the $2\,^1S_0$ metastable atoms. The channel numbers are for detector 1; the data for detector 2 have been averaged over velocity intervals whose width is determined by the channel width at detector 1.

channels. The display of Fig. 6 has 200 80-μsec-wide channels for each time-of-flight distribution and represents the sum of 10^5 separate data collection cycles during a total time of about 2 h; the vertical scale is about 10^5 counts/cm.

After being punched onto cards, the four time-of-flight distributions are analyzed to determine the $2\,^1S_0$ metastable state lifetime. The first step in the analysis is to obtain the distribution of $2\,^1S_0$ atoms by subtracting for each detector the data distribution for quench lamp on from that with the lamp off. Since the background counts at each detector are the same for lamp on as for lamp off, this subtraction of the two original distributions has an added dividend—the elimination of any background from the $2\,^1S_0$ distribution.

Next, the analysis program matches, for equal velocity intervals, the data from detector 1 with those from detector 2. Allowing the channel width at detector 1 to determine the velocity interval, a five-point Lagrange interpolation method is used to obtain the integral of the distribution at detector 2 for the same velocity interval. The result of this integration is illustrated for a 12-h run in Fig. 7, where the time-of-flight distributions for the $2\,^1S_0$ metastable atoms are plotted for both detectors.

Now that each distribution point for both detectors

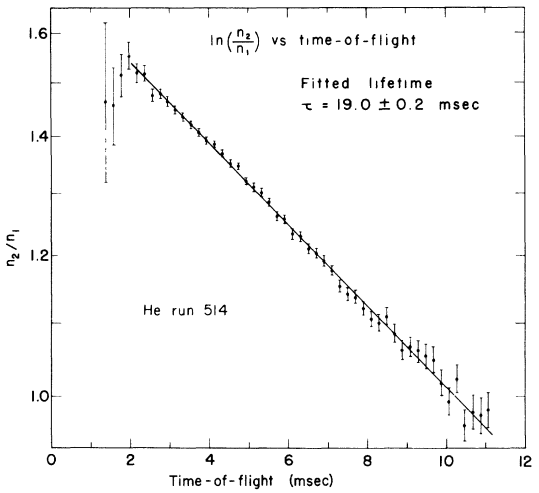

FIG. 8. 2^1S_0 decay plot. The ratio of detector 2 to detector 1 2^1S_0 metastable atom distributions versus the time of flight between detectors is a straight line on a logarithmic plot. The mean life τ of the 2^1S_0 state is obtained from the slope $= -1/\tau$ of the least-squares-fitted straight line; the fit only includes points which have counts equal to at least 10% of the number in the peak of the distribution.

corresponds to 2^1S_0 atoms with the same velocity, the ratio of detector 2 data to detector 1 data is taken. A straight line is then least-squares fitted to the natural logarithm of this ratio since, according to Eq. (10), $\ln R$ versus time of flight t is a straight line. The mean life τ of the 2^1S_0 metastable state is obtained from the slope $= -1/\tau$ of this fitted line. Figure 8 is a plot of $R(t)$ on a logarithmic scale versus time of flight t; the straight line is fitted only between data points that have a number of counts at least 10% of the number in the peak.

For each run the quench-lamp-on data, consisting almost entirely of 2^3S_1 metastable atoms, is also analyzed. Before the time-of-flight distributions are analyzed, however, a constant background is subtracted from each; for detector 1, this background is estimated from the counts collected in the last 10 channels on the long tail of the distribution, while for detector 2 the beginning channels, before any metastable atoms arrive, furnish the background information.

Since the 2^3S_1 state lifetime is expected to be essentially infinite compared to the flight times in our apparatus, a determination of the effective lifetime for this state serves as a very sensitive test of possible systematic errors in the data analysis. Also, an experimental estimate of about 1 sec is obtained as a lower limit for the 2^3S_1 state lifetime.

VII. RESULTS

A. Systematic Effects

During the course of the experiment, numerous parameters were varied in an attempt to discover any possible source of systematic error. Since an earlier version[13] of the apparatus had been limited both by insufficient drift-region vacuum and by inadequate buffer chambers, the present version was constructed with emphasis on the vacuum system. As a consequence, a factor of 10 increase in either the drift-region pressure or the beam flow rate over normal operating conditions produced no detectable change in the measured value of the lifetime to within the statistical accuracy of the experiment.

As pointed out in Sec. IV, the result for the mean life is expected to be independent of the initial velocity distribution. To examine this assertion, the source was operated with both liquid-nitrogen and liquid-helium cooling, although the close proximity of the source slit to the hot filament of the electron gun limited the actual source temperature to a value somewhat higher than that of the liquid coolant. Again no systematic effect on the lifetime result was observed. Unfortunately, operation of the source at room temperature did not furnish additional information because the statistical fit to the decay plot was poor; the higher beam velocity did not allow a time of flight sufficient for a significant amount of radiative decay to occur.

Another assertion of Sec. IV subject to experimental verification is that the fraction of 2^1S_0 atoms quenched by the lamp does not affect the lifetime measurement. When a neutral density screen was used to reduce the lamp intensity so that only about 50% of the 2^1S_0 atoms were quenched, the measured lifetime was the same, to within the statistical error, as for the fully quenched beam. Moreover, reducing the quench-lamp intensity also changes the 2^1S_0 time-of-flight distribution; the quenching fraction $f(v)$ appearing in Eq. (9) is velocity dependent, since the slower 2^1S_0 atoms, requiring more time to traverse the quench region, are preferentially quenched. Thus, lack of a systematic lamp intensity effect lends additional support to the conclusion that the lifetime measurement is independent of the initial velocity distribution.

Other parameters, such as distance of the source to the electron gun, electron-gun voltage, detector voltages, and channel width, were also varied with no effect. The extremely small solid angle subtended by the detectors excludes any significant contribution to the count rate from uv photons originating from either the quench region or from radiative decay. In addition, the retarding influence of gravity can be shown to be negligible for the ex-

perimental time of flight of even the slowest atoms.

However, one systematic effect, related to the source position and electron beam orientation, was found which could give at least a factor of 2 variation in the measured lifetime. Before this effect was discovered, the original configuration in the source region was a pinhole source and an electron beam perpendicular to the atomic beam; but with this particular arrangement, a 0.25-cm movement of the source hole perpendicular to the atomic beam direction would produce this large systematic effect. The explanation is contained in Eq. (4); it is absolutely essential that each position on the detector surface see the same velocity distribution. This condition is not necessarily true with a perpendicular electron beam, since different positions on the detector surface observe the electron bombardment region at different metastable atom recoil angles. In fact, one of the earliest experiments[20] on a metastable atom discusses the modification of the original velocity distribution following electron excitation to the metastable state. And, in agreement with this earlier work, the metastable velocity distribution in the present experiment, being well approximated by a v^6 dependence, is much faster than the distribution usually expected for effusion from a slit source.[21]

An attempt to assure that each position on the detector surface sees the same velocity distribution resulted in the final arrangement—a slit source and an electron beam antiparallel to the atomic beam. Although this configuration almost eliminates any systematic source position effect, the remaining uncertainty is a major contribution to the final error of the $2\,^1S_0$ lifetime measurement.

Finally, it is interesting to point out that, with the source hole on axis, the original source–electron-gun configuration gave the same measured lifetime as the final arrangement.

B. Errors

Compared to two other sources of error, the statistical error is sufficiently small that it does not contribute to the final error. The first significant error arises from the systematic source position effect already discussed. We shall take the size of this error to be equal to the change in the measured lifetime when the source slit is moved a distance equal to the slit length. The slit length is 0.5 cm, and a 0.5-cm movement parallel to its length and perpendicular to the atomic beam direction changes the lifetime by 1.2 msec. Therefore the systematic source position error is ± 0.6 msec.

The other major source of error occurs because the electron bombardment region extends for 1 cm along the atomic beam direction. This leads to an uncertainty in the velocity interval over which the detector 2 distribution is integrated, since the finite bombardment region results in an uncertainty in the effective distance to the two detectors. Taking one-half the bombardment length as the total distance error, a ± 0.25-cm change of the distances used in the data analysis program gives a subsequent error in the $2\,^1S_0$ lifetime of ± 0.4 msec. Combining this distance error with the systematic source position error yields a final error of ± 1.0 msec.

C. $2\,^1S_0$ Lifetime

Although over 200 runs were taken during the investigation of systematic effects, the final result for the $2\,^1S_0$ lifetime is based on 23 2-h runs and also on 3 12-h runs for He^4, and on 13 4-h runs for He^3. The lifetime result is essentially the same for both He^3 and He^4. The weighted average of these runs is 19.7 msec, with a statistical error of ± 0.1 msec. However, a consideration of the two major systematic errors in this experiment gives a final result of 19.7 ± 1.0 msec as the mean life of the $2\,^1S_0$ metastable state of helium.

---

†Based on a thesis submitted by Robert S. Van Dyck, Jr. to the Graduate Division, University of California, Berkeley, 1970, in partial fulfillment of the requirements for the Ph.D. degree. Work supported by the U.S. Atomic Energy Commission.

*Present address: Department of Physics, University of Washington, Seattle, Wash. 98105.

[1]I. S. Bowen, Astrophys. J. 67, 1 (1928).

[2]Maria Goeppert-Mayer, Ann. Physik 9, 273 (1931).

[3]G. Breit and E. Teller, Astrophys. J. 91, 215 (1940).

[4]L. Spitzer, Jr. and J. L. Greenstein, Astrophys. J. 114, 407 (1951).

[5]Lawrence H. Aller, *Astrophysics: Nuclear Transformations, Stellar Interiors, and Nebulae* (Ronald, New York, 1954), pp. 144–148.

[6]M. Lipeles, R. Novick, and N. Tolk, Phys. Rev. Letters 15, 690 (1965); 15, 815 (1965).

[7]D. R. Hamilton, Phys. Rev. 58, 122 (1940).

[8]A. Dalgarno, Monthly Notices Roy. Astron. Soc. 131, 311 (1966).

[9]A. Dalgarno and G. A. Victor, Proc. Phys. Soc. (London) 87, 371 (1966).

[10]G. A. Victor, Proc. Phys. Soc. (London) 91, 825 (1967).

[11]G. W. F. Drake, G. A. Victor, and A. Dalgarno, Phys. Rev. 180, 25 (1969).

[12]Verne Jacobs, Phys. Rev. A 4, 939 (1971).

[13]Murray Steinberg, Lawrence Radiation Laboratory Report No. UCRL-18387, 1968 (unpublished); Murray Steinberg and H. A. Shugart, Bull. Am. Phys. Soc. 14, 32 (1969).

[14]A. S. Pearl, Phys. Rev. Letters 24, 703 (1970).

[15]R. S. Van Dyck, Jr., C. E. Johnson, and H. A. Shugart, Phys. Rev. Letters 25, 1403 (1970).
[16]D. R. Bates, *Atomic and Molecular Processes* (Academic, New York, 1962), p. 3.
[17]G. Feinberg and J. Sucher, Phys. Rev. Letters 26, 681 (1971); G. W. F. Drake, Phys. Rev. A 3, 908 (1971).
[18]F. M. J. Pichanick, R. D. Swift, C. E. Johnson, and V. W. Hughes, Phys. Rev. 169, 55 (1968).
[19]F. D. Colegrove and P. A. Franken, Phys. Rev. 119, 680 (1960).
[20]W. E. Lamb, Jr. and R. C. Retherford, Phys. Rev. 79, 549 (1950).
[21]P. Kusch and V. W. Hughes, in *Encyclopedia of Physics*, edited by S. Flügge (Springer, Berlin, 1959), Vol. 37, Pt. 1, p. 3.

PHYSICAL REVIEW A VOLUME 4, NUMBER 4 OCTOBER 1971

Atomic Bethe-Goldstone Calculations of Term Splittings, Ionization Potentials, and Electron Affinities for B, C, N, O, F, and Ne

C. M. Moser
CECAM, Batiment 506, 91-*Campus* d'*Orsay, France*

and

R. K. Nesbet*
IBM Research Laboratory, San Jose, California 95114
(Received 21 May, 1971)

The ionization potentials, electron affinities, and term splittings of the lowest electronic configurations for first-row atoms for Z from 5 to 10 have been computed. The method used is that applied previously to ground-state correlation energies. Variational calculations equivalent to solution of one- and two-particle Bethe-Goldstone equations are carried out, following approximate Hartree-Fock calculations for each state of each atom or ion considered. Computed quantities are in reasonably good agreement with experiment. Bethe-Goldstone equations as used here are defined in terms of individual orbital excitations. Calculations of three-particle effects are included in some cases, computed with less relative accuracy than the other results. The three-particle terms are not negligible. In particular, they substantially reduce the magnitude of computed electron affinities.

I. INTRODUCTION

In this paper, results are presented using the variational solution of one- and two-particle Bethe-Goldstone equations[1] to examine the importance of electronic correlation effects in three physically important problems: (i) term splitting in the same configuration; (ii) successive ionization potentials; and (iii) electron affinities of neutral atoms. In each case, the quantity of interest is an energy difference, to which the difference of valence-shell correlation energies can make a substantial contribution.

Results will be given for atoms and ions with the configuration $1s^2 2s^2 2p^N$, where N ranges from 1 to 6 and Z from 5 to 10.

The computational procedure (orbital-excitation Bethe-Goldstone equations) and its advantages and shortcomings have been discussed at length in several publications.[1-3] Several points only need to be mentioned here.

Bethe-Goldstone equations, as used in the present calculations, are defined in terms of virtual excitations of individual spin orbitals. The variational trial function for one-particle terms contains, together with the Hartree-Fock determinant or determinants, only Slater determinants in which precisely one occupied orbital has been replaced (single virtual excitation). Similarly, two-particle terms are computed with a trial function that contains single and double virtual excitations only. Symmetry-adapted wave functions, eigenfunctions of $\vec{L}^2$ and $\vec{S}^2$, cannot in general be constructed from such trial functions.

An alternative procedure is to use symmetry-adapted functions throughout. This can be accomplished by redefining the hierarchy of n-particle Bethe-Goldstone equations in terms of virtual excitations of *configurations* rather than of individual spin orbitals.[3] All virtual orbital excitations that involve the same relative change of (nl) quantum numbers must be included together in the variational trial function. Because a replacement such as $2p_1^\alpha / 2p_{-1}^\alpha$ would not change (nl), configurational excitations of a given order involve orbital excitations that are nominally of higher orders. Thus the trial function for a one-electron *configurational* Bethe-Goldstone calculation contains terms that would first occur in two-electron or three-electron *orbital* Bethe-Goldstone calculations.

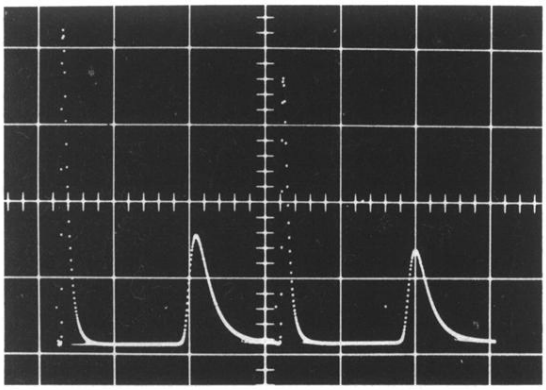

FIG. 6. Interface oscilloscope display. The first half of the display, consisting of 200 80-μsec-wide channels for each detector, corresponds to the quench lamp off, while the second 400 channels are with the lamp on. The decrease in peak height represents the $2\,^1S_0$ metastable atoms that are quenched by the discharge lamp. The vertical scale is about 10^5 counts/cm.